Note:

Comments on "The sensitivity study of radiative-convective equilibrium in the Tropics with a convective resolving model"

by

W.-K. Tao[1], C.-L. Shie[1,2] and J. Simpson[1]

[1] *Laboratory for Atmospheres*
[2] *Science Systems and Applications Inc.*

NASA/Goddard Space Flight Center
Greenbelt, MD 20771

J. of Atmos. Sci.

(February 1, 2000)

Corresponding author address: Dr. Wei-Kuo Tao, Mesoscale Atmospheric Processes Branch, Code 912, NASA/GSFC, Greenbelt, MD 20771
email: tao@agnes.gsfc.nasa.gov

1. Introduction

In general, there are two broad scientific objectives when using cloud resolving models (CRMs or cloud ensemble models-CEMs) to study tropical convection. The first one is to use them as a physics resolving models to understand the dynamic and microphysical processes associated with the tropical water and energy cycles and their role in the climate system (Sui *et al.* 1994; Grabowski *et al.* 1996; and others listed in Table 1 in Tao *et al.* 1999). The second approach is to use the CRMs to improve the representation of moist processes and their interaction with radiation in large-scale models (see GEWEX Cloud System Study, GCSS, Plan, 1993). In order to improve the credibility of the CRMs and achieve the above goals, CRMs using identical initial conditions and large-scale influences need to produce very similar results.

Two CRMs produced different statistical equilibrium (SE) states (warm and humid in Grabowski *et al.* 1996 and cold and dry in Sui *et al.* 1994) even though both used the same initial thermodynamic and wind conditions (1956 Marshall Islands data). Tao *et al.* (1999) have performed sensitivity tests to identify the major physical processes that determine the SE states for the different CRM simulations. Their results indicated that atmospheric horizontal wind is treated quite differently in these two CRMs. The model that had *stronger surface winds* and consequently larger latent and sensible heat fluxes from the ocean produced a warmer and more humid modeled thermodynamic SE state. In addition, Tao *et al.* (1999) found that the domain mean thermodynamic state is more unstable for those experiments that produced a warmer and more humid SE state.

Xu and Randall (1999), however, indicated that their simulated wet (warm and humid) SE states are thermally more stable in the lower troposphere (from the surface to 4-5 km in altitude). Xu and Randall (1999) also suggested that the large-scale horizontal advective effects on temperature and water vapor mixing ratio (ignored in Tao *et al.* 1999 and others) are needed when using CRMs to perform long-term integrations to study convective feedback under specified large-scale environments. In addition, they suggested that the dry and cold SE state simulated by Sui *et al.* (1994) was caused by enhanced precipitation but not enough surface evaporation. We find some problems with their interpretation of these three phenomena.

2

2. Comments

2.1 *Large-scale forcing employed in the CRMs*

The observed large-scale advective forcing in temperature and water vapor can be imposed into CRMs as first suggested by Soong and Ogura (1980) and Soong and Tao (1980). In general, there are two ways to implement large-scale advective forcing in the CRM as suggested by Soong and Tao (1980) and are shown in the following equations for water vapor mixing ratio (with a similar equation for the potential temperature).

$$\left[\frac{\partial \overline{q}_v}{\partial t}\right]_{L.S.} = -[\overline{w}]_{Observed}\left[\frac{\partial \overline{q}_v}{\partial z}\right]_{Modeled} \tag{1}$$

$$\left[\frac{\partial \overline{q}_v}{\partial t}\right]_{L.S.} = -\left[\vec{v} \cdot \nabla \overline{q}_v - \overline{w}\frac{\partial \overline{q}_v}{\partial z}\right]_{Observed} \tag{2}$$

One is to specify the large-scale vertical velocity ($\overline{w}$, derived from observations) in the model and compute the advective forcing in temperature and water vapor using the model mean vertical temperature and water vapor gradients (adopted by Sui *et al.* 1994; Grabowski *et al.* 1996 and Tao *et al.* 1999). This method is physically realistic by allowing more explicit interaction between prescribed large-scale velocity and convection and its interactive processes with radiation and surface fluxes. In the second approach, the observed large-scale advective forcing can be held constant during the model integration (adopted by Xu and Randall, 1999). The second approach has the advantage of fixed/observed large-scale forcing, and would make comparisons with observations more meaningful. This approach should be used if one is interested in using the model output to improve the representation of cumulus parameterization in large-scale models (GCSS). The second approach can also provide high temporal and spatial distributions of cloud information that can not be measured easily. However, the second approach requires a detailed comparison between observations and model simulations (Moncrieff *et al.* 1997 and Moncrieff and Tao, 1999).

Xu and Randall (1999) performed two numerical experiments, cM (the second approach) and cW (the first approach), to identify the importance of the large-scale horizontal advective effects on temperature and water vapor mixing ratio in their simulated SE states. The cM experiment produced a thermodynamic SE state that was closer to a 3 month observed mean thermodynamic state than that of the cW experiment (see Fig. 1)[1]. Xu and Randall (1999) then used the relatively poor performance of the cW experiment to identify the important role of the large-scale horizontal advective effects upon their simulated SE states. As shown in (1) and (2), experiment cW is not the same as the experiment without large-scale horizontal advective effects. Xu and Randall (1999), however, never performed a numerical experiment without the large-scale horizontal advective effects on temperature and water vapor. They also did not separate the vertical and the horizontal components in the large-scale forcing to show the relative magnitude of horizontal component to the total forcing (shown in their Fig. 2a). We feel that their results may be misleading and can not be used to address the importance of large-scale horizontal advective effects on temperature and water vapor in their own or other CRM studies (for understanding the dynamic and microphysical processes associated with the tropical water and energy cycles and their role in the climate system).

Xu and Randall (1999) also stated that the model used by Sui *et al.* (1994) does not have the *ability* to maintain the initial wind profile. As discussed in Tao *et al.* (1999), the Sui *et al.* (1994) model set-up did not add any artificial terms (i.e., nudging or other) to the horizontal (u) momentum equation that would maintain the domain mean horizontal (u) momentum close to its initial value. Consequently, the horizontal momentum is simply mixed by convective transport processes in Sui *et al.* (1994) resulting in weak surface wind speeds and almost uniform horizontal flow through the whole troposphere after 4 days of the model integration. We feel that the ideal design for future CRM simulations should allow both convective mixing and large-scale processes involving the horizontal momentum by allowing for the change in strength and vertical shear of horizontal momentum. This could be particularly important in any CRM simulation allowing time-varying large-scale vertical motion (Experiments, vW, vhW and vG-ns, in Xu and Randall (1999)).

---

1 Soong and Tao (1980), Tao and Soong (1986), Krueger (1988), Grobowski *et al.* (1999), Li *et al.* (1999) and many others have shown that any CRM with reasonable physics shall produce results in good agreement with observations if observed large-scale advective forcing is super-imposed into the CRM as a main forcing.

2.2 *Moisture Budget and Physical Processes Determined the CRM Simulated SE states*

Tao *et al.* (1999) and Xu and Randall (1999) both examined the domain averaged temperature and water vapor budgets to identify the physical processes that determined the different CRM simulated SE states. For example, the water vapor (q_v) budget can be integrated over the horizontal and from the surface to the top of the model domain to yield

$$L_v < \frac{\partial \bar{\rho}\bar{q}_v}{\partial t} > = -< L_v\bar{\rho}(\bar{c}-\bar{e}) + L_s\bar{\rho}(\bar{d}-\bar{s}) > + L_v < \bar{\rho}[\frac{\partial \bar{q}_v}{\partial t}]_{L.S.} > + L_v\bar{E}_o \qquad (3)$$

where c, e, d and s are condensation, evaporation, deposition and sublimation, of cloud, respectively[2]. $L_v < \bar{\rho}[\frac{\partial \bar{q}_v}{\partial t}]_{L.S.} >$ is the imposed large-scale advective moistening ((1) or (2)); $\bar{\rho}$ is air density; and E_o is the latent heat flux from the ocean surface. The variables L_v and L_s are the latent heats of condensation and sublimation, respectively.

Tao *at al.* (1999) identified the physical processes responsible for determining the modeled equilibrium states by examining the budget differences between CRM simulated warm/humid and cold/dry SE states. Table 1 lists individual components of the water vapor budget[3] simulated by Xu and Randall (1999) and Tao *et al.* (1999). The difference in precipitation between experiments cW and vW in Xu and Randall (1999) is very small. These two runs can not be used to justify that the dry and cold SE state was caused by enhanced precipitation but not enough surface evaporation. The difference between experiments cW and cM is very large, but both surface evaporation and large-scale advective forcing in water vapor contribute equally for their difference in precipitation. Therefore, Xu and Randall's suggestion that the dry and cold SE state was caused by enhanced precipitation but not enough surface evaporation is not justified.

---

2 The net condensation, $< L_v\bar{\rho}(\bar{c}-\bar{e}) + L_s\bar{\rho}(\bar{d}-\bar{s}) >$, almost equals the surface precipitation (LP in Xu and Randall, 1999) in a long term integration.

3 It is not clear why the local change term in the water vapor budget is zero in Xu and Randall (1999).

Several noted differences between Tao *et al.* (1999) and Xu and Randall (1999) can be seen in Table 1. For example, the runs that produced the more humid (drier) SE states are always associated with larger (smaller) latent heat flux from the ocean, larger (smaller) net condensation and larger (smaller) large-scale advective forcing in Tao *et al.* (1999). It implies that more surface latent heat fluxes and large-scale advective forcing in water vapor can allow/cause more net condensation/surface precipitation. By contrast, the relative warm/humid SE state (experiment cW) in Xu and Randall (1999) is associated with less latent heat flux from the ocean, less net condensation and less large-scale advective forcing than the relatively cold/dry SE state (experiment cM). Also, note in Table 1 that the contribution of the large-scale advective forcing in water vapor to net condensation/surface precipitation ranges from 0.67 to 0.70 in Xu and Randall (1999) for their Marshall Island simulations. It is about 0.81 to 0.85 in Tao *et al.* (1999) and Sui *et al.* (1994). The GCE modeled precipitation processes have a stronger response to the large-scale advective forcing than the UCLA-CSU CEM (Xu and Randall, 1999). On the other hand, the surface latent heat fluxes only contribute to about 15-21% of the total precipitation processes (net condensation/surface precipitation) in the GCE model compared to 30-33% in the UCLA CSU CEM. Two models [the Goddard Cumulus Ensemble (GCE) Model and the UCLA-CSU CEM] behave very differently in terms of precipitation processes and their interaction with surface processes and the imposed large-scale advective forcing.

Tripoli's (1992) cloud resolving model used in Grabowski *et al.* (1996) also has a larger contribution from the large-scale forcing to the precipitation processes (81%) and a smaller ratio (19%) between surface latent heat fluxes and surface precipitation. Yanai *et al.* (1976) analyzed Marshall Islands (1956) data and found that the surface latent heat fluxes make up about 21.7% of the surface precipitation during disturbed periods (dominated by deep cumuli - Type 1 classification with 351 cases). The ratio between the latent heat fluxes and the surface precipitation increases to 37% for un-disturbed convective periods (shallow cumuli - Type 2 classification with 35 cases). The classification is based on observed large-scale vertical velocity (positive or upward for disturbed periods and negative or downward for undisturbed periods). The large-scale vertical velocity imposed in the CRMs is all upward and the modeled precipitation processes are quite active.

We believe that GCE model results are in very reasonable agreement with observations.

Another comment is that Xu and Randall (1999) performed several GATE simulations, and they indicated that the presence of vertical shear of the horizontal wind does not significantly change the simulated SE states, *provided that the surface wind speeds are identical.* These results are, somewhat, consistent with Tao *et al.* (1999) in that "*runs with stronger (weaker) surface winds produce more latent heat fluxes and warm and humid (cold and dry) SE states*". However, we feel that all of their GATE simulations may be inappropriate because the observed precipitable water during GATE Phase III never reaches an equilibrium state (see Fig. 15 in Xu and Randall, 1996). In addition, their GATE simulations did not employ observed large-scale advective forcing in temperature and water vapor.

2.3 *Stability in CRM Simulated Equilibrium States*

Figure 2(a) shows the relation between the surface relative humidity and the lower-tropospheric lapse rate (below the 4.7 km level) for a fixed sea surface temperature (SST, 28 ^{o}C). The results show a negative correlation between surface relative humidity and the lower troposheric lapse rate. The results in Fig. 2(a) show that warm/humid SE states are thermally more stable and cold/dry SE states are thermally more unstable in the lower troposphere in both Xu and Randall (1999) and Tao *et al.* (1999) .

Figure 2(b) shows the relation between the surface relative humidity and the lapse rate for "*equivalent potential temperature*" (an indicator for Convective Available Potential Energy - CAPE). The results shown in Fig. 2(b) indicate that the thermodynamic state is more unstable (stable) for those experiments that produced a warmer and more humid (cold and dry) SE state. In addition, the domain column mean thermodynamic profile has a stronger vertical gradient of water vapor for those experiments that produced warmer and more humid SE states compared to the experiments that produced colder and drier SE states. This is why stronger large-scale forcing (the first approach) can lead to the larger heating/moistening in the local temporal change of temperature and water vapor in Tao *et al.* (1999) (see Table 1). Our results also indicated that warmer and more humid SE states are associated with a larger CAPE (2000 to 2500 $m^2 s^{-2}$) compared to the colder and drier SE states (1300 to 1600 $m^2 s^{-2}$).

3. Summary

Xu and Randall (1999) performed sensitivity tests to improve the understanding of radiative-convective equilibrium in the tropics using the UCLA-CSU CEM. We have three major comments on their three major conclusions:

1) Xu and Randall (1999) did not show solid evidence of the important role of large-scale horizontal advective forcing in temperature and water vapor on their simulated SE states. Although, we do feel that horizontal advective forcing is needed when a CEM is used for comparison with observations and for the purposes of the GCSS (to improve the understanding of moist processes in General Circulation Models and Climate Models).

2) Their interpretation of Sui *et al.*'s (1994) results that the dry and cold SE state was caused by enhanced precipitation but not enough surface evaporation can not be justified, because their own CEM simulations clearly indicated that both surface evaporation and large-scale advective forcing of water vapor contribute equally to the difference in precipitation. Also, their simulated warm/humid SE states are associated with less surface precipitation/net condensation, less large-scale advective forcing and less latent heat fluxes from the ocean compared to the cold/dry SE states. By contrast, the warm/humid (cold/dry) SE states simulated by Tao *et al.* (1999) are characterized with more (less) surface precipitation, more (less) large-scale advective forcing and more (less) surface fluxes. In addition, their CEM's precipitation processes have a weaker response to the imposed large-scale advective forcing in water vapor but a larger contribution from surface latent heat fluxes to surface precipitation as compared to two other CEMs (Goddard Cumulus Ensemble Model and Tripoli, 1992) even though all the models were initialized with the same data from the Marshall Islands (1956). The GCE and Tripoli's model results are in good agreement with observations (Yanai *et al.* 1976).

3) Their warm/wet SE states are more stable than their corresponding cold/dry SE states in lower troposphere. They only discussed the vertical stability (lapse rate) of a dry atmosphere. However, the warm/wet SE states are actually more unstable (lapse rate of equivalent potential temperature or wet-bulb potential

temperature) in lower troposphere than their corresponding cold/dry SE states. In addition, the warm/wet SE states are always associated with higher Convective Available Potential Energy than their corresponding cold/dry SE states.

In order to use the CRM as a physical-process resolved model to understand the dynamic and microphysical processes associated with tropical water and energy cycles and their role in the climate system, we need to use available observations to validate whether a warm and humid thermodynamic state (i.e., ENSO) is associated with stronger large-scale advective forcing (i.e., large-scale moisture convergence) and larger surface fluxes from the oceans than its counterpart cold and dry state. We also can use observationscould to address whether or not the CAPE is higher for a simulated warm/humid SE than that associated with a cold/dry SE. The design (i.e., time-variant large-scale forcing in temperature and water vapor, and horizontal momentum) of future CRMs for studying convective-radiative equilibrium in the tropics needs to be addressed.

4. Acknowledgement

The authors thank Mr. S. Lang, Dr. B. Ferrier and Dr. C.-H. Sui for reading the manuscript. We also thank Drs. R. Adler and W. Lau for discussions related to rainfall observation. This work is supported by the NASA Headquarters Physical Climate Program, the NASA Tropical Rainfall Measuring Mission (TRMM) and the Interdisciplinary Investigation of the Earth Observing System (EOS). These authors are grateful to Dr. R. Kakar for his support of this research. Acknowledgment is also made to NASA/Goddard Space Flight Center for computer time used in the research.

5. References

GEWEX Cloud System Science Team, 1993: The GEWEX Cloud System Study (GCSS). *Bull. Amer. Meteor. Soc.*, **74**, 387-399.

Grabowski, W. W., M. W. Moncrieff, and J. T. Kiehl, 1996: Long-term behavior of precipitating tropical cloud systems: A numerical study. *Quart. J. Roy. Meteor. Soc.*, **122**, 1019-1042.

Johnson, D., W.-K. Tao, J. Simpson, and C.-H. Sui, 2000: A Study of the Response of Deep Tropical Clouds to Large-Scale Processes, Part I: Model Set-up Strategy and Comparison with observation. *J. Atmos. Sci.*, (submitted).

Krueger, S. K., 1988: Numerical simulation of tropical cumulus clouds and their interaction with the subcloud layer. *J. Atmos. Sci.*, **45**, 2221-2250.

Li, X., C.-H. Sui, K.-M. Lau and M.-D. Chou, 1999: Large-scale forcing and cloud-radiation interaction in the tropical deep convective regime. *J. Atmos. Sci.*, **56**, 3028-3042.

Moncrieff, M. W., S. K. Krueger, D. Gregory, J.-L. Redelsperger and W.-K. Tao, 1997: GEWEX Cloud System Study (GCSS) Working Group 4: Precipitating convective cloud systems. *Bull. Amer. Meteor. Soc.*, **78**, 831-845.

Moncrieff, M. W., and W.-K. Tao, 1999: Cloud-resolving models. Global Water and Energy Cycles, Chapter 5, Ed. by K. Browing and R. J. Gurney, *Cambridge University Press*, 200-209.

Soong, S.-T., and Y. Ogura, 1980: Response of tradewind cumuli to large-scale processes. *J. Atmos. Sci.* , **37**, 2035-2050.

Soong, S.-T., and W.-K. Tao, 1980: Response of deep tropical clouds to mesoscale processes. *J. Atmos. Sci.*, **37**, 2016-2036.

Sui, C. H., K. M. Lau, W.-K. Tao, and J. Simpson, 1994: The tropical water and energy cycles in a cumulus ensemble model. Part I: Equilibrium climate. *J. Atmos. Sci.*, **51**, 711-728.

Tao, W.-K., and S.-T. Soong, 1986: A study of the response of deep tropical clouds to mesoscale processes: Three-dimensional numerical experiments. *J. Atmos. Sci.*, **43**, 2653-2676.

Tao, W.-K., J. Simpson, C.-H. Sui, C.-L. Shie, B. Zhou, K. M. Lau, and, M. Moncrieff, 1999: On equilibrium states simulated by Cloud-Resolving Models, *J. Atmos. Sci.*, **56**, 3128-3139.

Tripoli, G. J., 1992: A nonhydrostatic mesoscale model designed to simulate scale interaction. Mon. Wea. Rev., 120, 1342-1359.

Xu, K.-M and D. A. Randall, 1996: Explicit simulation of cumulus ensembles with the GATE Phase III data: Comparison with observations. *J. Atmos. Sci.*, **53**, 3710-3736.

Xu, K.-M., and D. A. Randall, 1999: A sensitivity study of radiative-convective equilibrium in the tropics with a convective-resolving model. *J. Atmos. Sci.*, **56**, 3385-3399.

Yanai, M., J.-H. Chu, T. E. Stark and T. Nitta, 1976: Response of deep and shallow tropical maritime cumuli to large-scale processes. *J. Atmos. Sci.*, **33**, 976-991.

Figure Captions

Fig. 1 Scatter plot of horizontal mass-weighted temperature vs water vapor after 25 days of integration from GCE model (Runs 1 to 4 and Runs 1W to 4W) and UCL-CSU CEM simulations (using the same data from Marshall Islands). The result from Sui *et al.* (1994) after 25 days of integration is denoted as **S** while that of Grabowski *et al.* (1996) is denoted as **G**. Observations from TOGA COARE (**TC**) and Marshall Islands (**MI**) regions are shown. **cM, cW** and **vW** are from Xu and Randall (1999). Runs 1W to 4W are the runs that produced warm/humid SE state similar to Grabowski *et al.* (1996) (grouped with G in the same box). Runs 1 and 2 are centered at 259 K and 57 mm and they grouped with cM in the same box. Runs 3 and 4 are the runs produced very cold and dry SE state.

Fig. 2 **(a)** Scatter diagram of surface relative humidity and the lower-tropospheric lapse rate after 25 days of the GCE model simulations. **(b)** is the same as **(a)** expect equivalent potential lapse rate (an indicator of stability).

Table Captions

Table 1 Individual terms of the column moisture budget for SE states simulated in Xu and Randall (1999) and Tao *et al.* (1999). Note that the $\mathbf{L_vP}$ is the net condensation (sum of condensation, deposition, evaporation and sublimation of cloud). $L_v < \bar{\rho}[\frac{\partial \bar{q}_v}{\partial t}]_{L.S.} >$ is the imposed large-scale advective effect on water vapor, and $L_v < \frac{\partial \bar{\rho} \bar{q}_v}{\partial t} >$ is the local time change of water vapor. Units are W m^{-2}. Differences in the individual moisture budget terms for Run cW (warm and humid) and Runs vW and cM are also shown. *The local change term is zero in Xu and Randall (1999) and we used their Fig. 10 to approximately estimate the difference between cW and cM, and cW and vW.

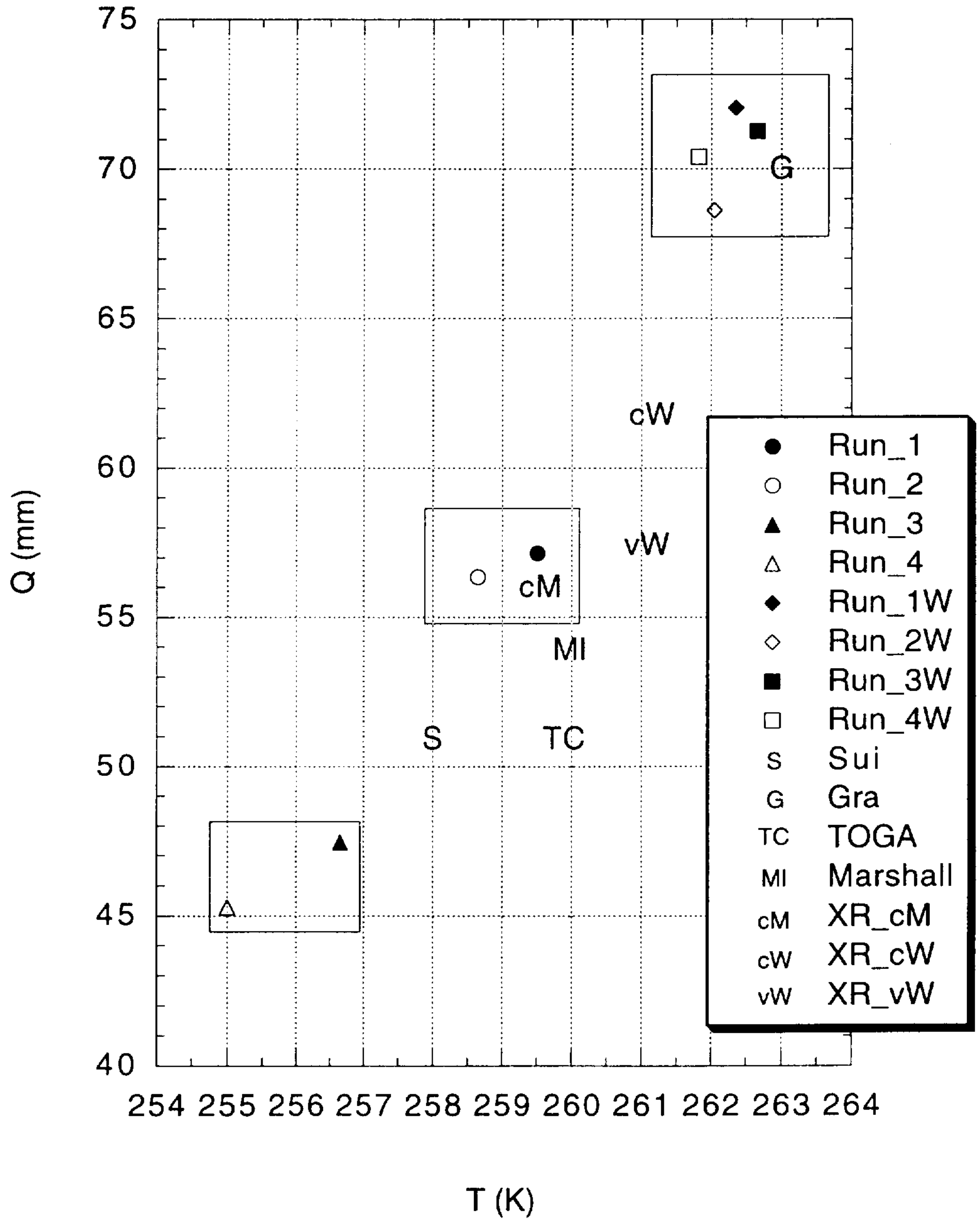

75
70
65
60
55
50
45
40
254 255 256 257 258 259 260 261 262 263 264
T (K)
Q (mm)
G
cW
vW
cM
MI
S
TC
Run_1
Run_2
Run_3
Run_4
Run_1W
Run_2W
Run_3W
Run_4W
S Sui
G Gra
TC TOGA
MI Marshall
cM XR_cM
cW XR_cW
vW XR_vW

Fig. 1

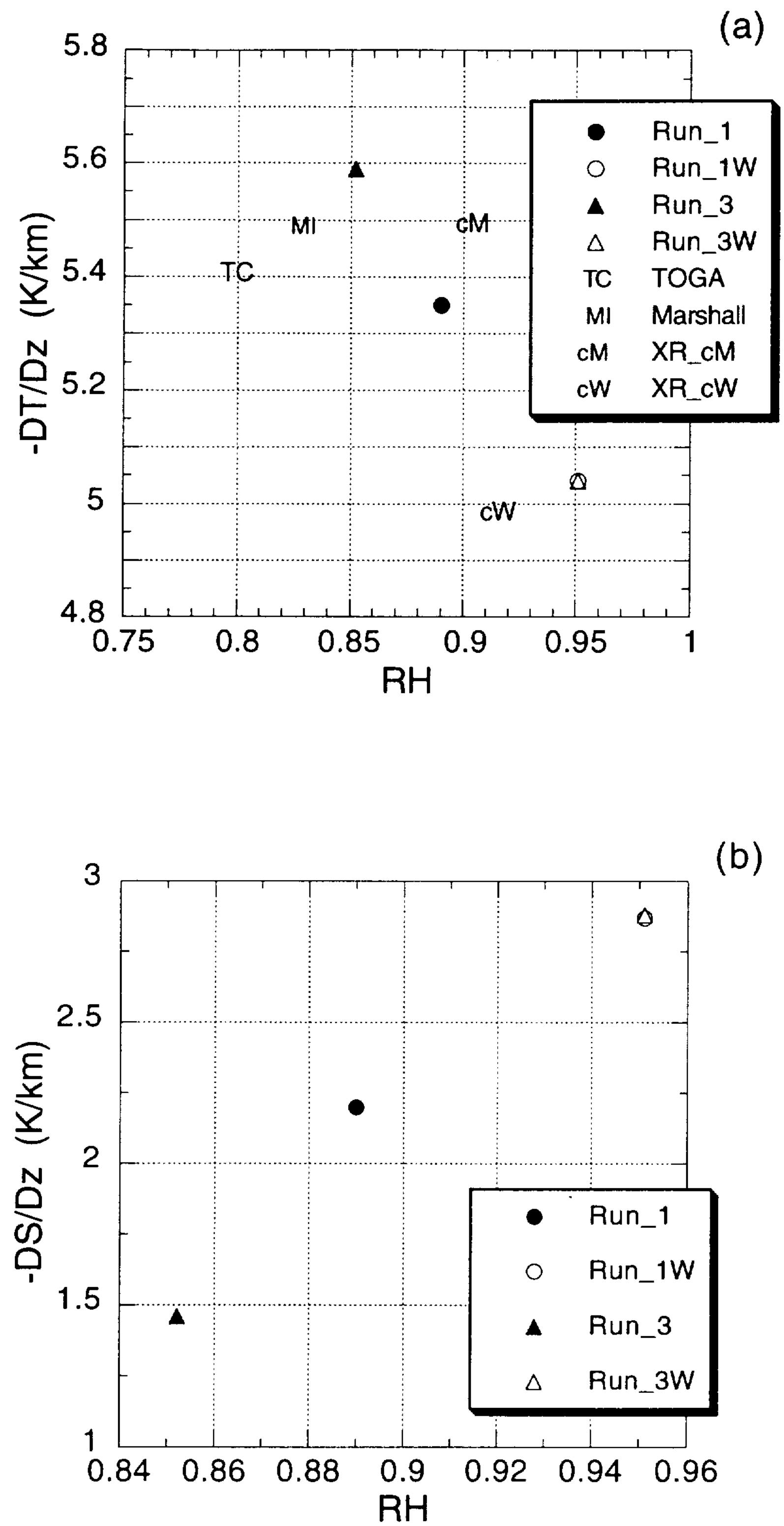

(a)
-DT/Dz (K/km)
RH
5.8
5.6
5.4
5.2
5
4.8
0.75
0.8
0.85
0.9
0.95
1
TC
MI
cM
cW
Run_1
Run_1W
Run_3
Run_3W
TC TOGA
MI Marshall
cM XR_cM
cW XR_cW
(b)
-DS/Dz (K/km)
RH
3
2.5
2
1.5
1
0.84
0.86
0.88
0.9
0.92
0.94
0.96
Run_1
Run_1W
Run_3
Run_3W

Fig. 2

Table 1

Experiment	$-L_vP$	L_vE_o	$L_v < \overline{\rho}[\frac{\partial \overline{q}_v}{\partial t}]_{L.S.} >$	$L_v < \frac{\partial \overline{\rho}\overline{q}_v}{\partial t} >$
cW	-398	118	280	0
v W	-402	133	269	0
cM	-456	145	311	0
Run 1	-502.4	97.8	410.6	5.89
Run 2	-490.2	97.8	397.8	5.35
Run 1W	-545.3	105.2	463.6	23.14
Run 2W	-536.8	110.2	446.5	19.35
cW - vW	4	-15	11	5.0*
cW - cM	58	-27	-31	6.7*